Cell, Vol. 108, 781–794, March 22, 2002, Copyright ©2002 by Cell Press

Hairpin Opening and Overhang Processing by an Artemis/DNA-Dependent Protein Kinase Complex in Nonhomologous End Joining and V(D)J Recombination

Yunmei Ma,[1] Ulrich Pannicke,[2] Klaus Schwarz,[2,3] and Michael R. Lieber[1,3]
[1]Norris Comprehensive Cancer Center, Rm. 5428
Departments of Biochemistry & Molecular Biology, Pathology, Biological Sciences, and Molecular Microbiology & Immunology
1441 Eastlake Avenue
Los Angeles, California 90033
[2]Department of Transfusion Medicine
University of Ulm
German Red Cross Blood Donation Service
Baden-Wuerttemberg-Hessen, Institute Ulm
Helmholtzstrasse 1D
D-89081 Ulm
Germany

Summary

Mutations in the Artemis protein in humans result in hypersensitivity to DNA double-strand break-inducing agents and absence of B and T lymphocytes (radiosensitive severe combined immune deficiency [RS-SCID]). Here, we report that Artemis forms a complex with the 469 kDa DNA-dependent protein kinase (DNA-PK$_{cs}$) in the absence of DNA. The purified Artemis protein alone possesses single-strand-specific 5′ to 3′ exonuclease activity. Upon complex formation, DNA-PK$_{cs}$ phosphorylates Artemis, and Artemis acquires endonucleolytic activity on 5′ and 3′ overhangs, as well as hairpins. Finally, the Artemis:DNA-PK$_{cs}$ complex can open hairpins generated by the RAG complex. Thus, DNA-PK$_{cs}$ regulates Artemis by both phosphorylation and complex formation to permit enzymatic activities that are critical for the hairpin-opening step of V(D)J recombination and for the 5′ and 3′ overhang processing in nonhomologous DNA end joining.

Introduction

V(D)J recombination is the process by which immunoglobulin and T cell receptor variable domain exons are assembled from V, D, and J elements in bone marrow pre-B cells and thymic pre-T cells, respectively (Fugmann et al., 2000; Grawunder et al., 1998a; Lewis, 1994). It is critical for the development of the immune system, and human patients deficient for this process manifest severe combined immune deficiency (SCID, see below; Schwarz et al., 1991, 1996; Vanasse et al., 1999; Villa et al., 2001). This site-specific recombination process occurs precisely at the end of each V, D, or J element (the coding end), where it is bordered by recombination signal sequences (RSS) that consist of a heptamer, a 12 or 23 bp spacer, and a nonamer (see Supplemental Figure S1 at http://www.cell.com/cgi/content/full/108/6/781/DC1). The RAG-1 and -2 proteins, along with HMG1 or 2, form a complex (the RAG complex) that binds at the heptamer/nonamer recombination signal sequences (designated 12- or 23-RSS, based on the spacer length) (Gellert, 1997). The RAG complex endonucleolytically nicks the DNA 5′ of the heptamer, where it borders each V, D, or J element. The 12- and 23-RSS synapse and the RAG complex then uses the 3′ hydroxyl (3′ OH) on each V, D, or J coding end as a nucleophile in a transesterification attack (van Gent et al., 1996) on the antiparallel DNA strand. A DNA hairpin is thus generated at each V, D, or J coding end, and the configuration of the signal end, where the RSS is located, is blunt.

Recombination events occurring within lymphoid cells require one 12-RSS and one 23-RSS; this feature is designated as the 12/23 rule. After the generation of the two hairpinned coding ends and the two signal ends, the four DNA ends appear to be held by the RAG complex in a postcleavage complex (Agrawal and Schatz, 1997; Hiom and Gellert, 1997). In order for the variable domain exon to be created, the V and J coding ends must each be released from their hairpin configuration. One of the major unresolved questions in V(D)J recombination concerns how the hairpinned coding ends are opened. This question can be assayed using DNA oligonucleotide hairpins (termed free hairpins), or it can be assayed using RAG-generated hairpins. It has been shown that the RAG complex can open free hairpins (Besmer et al., 1998). However, this activity of the RAG complex is only substantial in manganese ion-containing buffers, and it is not observed in magnesium ion-containing buffers. Many nucleases have altered specificities when provided with Mn^{2+}. Hence, these observations are interesting but may not be physiologically relevant.

Once the hairpins are opened, the joining phase of V(D)J recombination is carried out by the nonhomologous DNA end-joining pathway (NHEJ) (Lieber, 1999). This is the major DNA double-strand break repair pathway in somatic cells of all multicellular eukaryotes, and defects in this pathway result in sensitivity to DNA double-strand break-inducing agents (such as X-rays) in all somatic cells and failure to complete V(D)J recombination in lymphoid cells (van Gent et al., 2001). X-ray sensitivity, genetic, and biochemical studies have permitted the identification of several key proteins in the NHEJ pathway (Wood et al., 2001). Ku and the 469 kDa DNA-dependent protein kinase, DNA-PK$_{cs}$, each can bind independently to DNA ends (Hammarsten and Chu, 1998; West et al., 1998; Yaneva et al., 1997). However, upon Ku binding to a DNA end, Ku improves the affinity of DNA-PK$_{cs}$ for the DNA end by 100-fold (West et al., 1998). The crystal structure for Ku (Walker et al., 2001) and the lower-resolution structures for DNA-PK$_{cs}$ (Chiu et al., 1998; Leuther et al., 1999) are consistent with models in which each protein can bind at the transitions from single- to double-stranded DNA. Though DNA-PK$_{cs}$ is a DNA end-dependent serine/threonine protein kinase and though in vitro it can phosphorylate many polypeptides, its relevant phosphorylation targets in V(D)J re-

[3]Correspondence: lieber@usc.edu (M.R.L.), klaus.schwarz@medizin.uni-ulm.de (K.S.)

combination and in NHEJ have remained undefined (Anderson and Carter, 1996).

The two DNA ends generated at pathologic double-strand DNA breaks are rarely compatible. In the physiologic dsDNA breaks of V(D)J recombination, the coding end hairpins are suspected to be opened preferentially 3′ to the tip (Schlissel, 1998), resulting in only a minority of ends with terminal microhomology. The nucleases involved in trimming the ends and the polymerases involved in filling in any gaps in NHEJ have yet to be definitively identified. In *S. cerevisiae*, there is genetic evidence supporting the role of polymerase β in filling in a subset of the gaps and of FEN-1 in trimming some of the 5′ flaps (Wilson and Lieber, 1999; Wu et al., 1999). The necessary nucleases and polymerases involved in NHEJ of multicellular eukaryotes have not been identified (see Supplemental Figure S1 at http://www.cell.com/cgi/content/full/108/6/781/DC1).

The most well-understood phase of the NHEJ pathway is the ligation step, where it is clear that the ligase is DNA ligase IV in yeast, mice, and humans, and presumably in all eukaryotic organisms, including plants (Barnes et al., 1998; Gao et al., 1998; Grawunder et al., 1997, 1998b; Schar et al., 1997; Teo and Jackson, 1997; Wilson et al., 1997) (see Supplemental Figure S1). XRCC4 is a polypeptide that forms a heteromultimer with DNA ligase IV, is required in vivo, and is stabilizing and stimulatory for DNA ligase IV function (Grawunder et al., 1997; Modesti et al., 1999).

RAG mutations and NHEJ component null mutations have been found to result in a severe combined immune deficiency (SCID) (Schwarz et al., 1996; Vanasse et al., 1999; Villa et al., 2001). The mutations in the NHEJ pathway also result in sensitivity to agents that cause double-strand DNA breaks, such as X-rays and bleomycin. The most recently identified gene of which mutation results in X-ray sensitivity and in SCID is called *Artemis* (Moshous et al., 2001). The putative protein encoded by the *Artemis* gene only has limited homology to the SNM1 protein of *S. cerevisiae* and mouse, absence of which results in sensitivity to DNA interstrand crosslinking agents (Dronkert et al., 2000; Henriques and Moustacchi, 1980). Human cells deficient for Artemis have the same V(D)J recombination phenotype as murine DNA-PK_{cs} mutants (Bosma and Carroll, 1991; Hendrickson et al., 1991; Lieber et al., 1988; Moshous et al., 2001; Nicolas et al., 1998; Schuler et al., 1986). That is, signal joint formation occurs at normal or near-normal levels, whereas coding joint formation is reduced over 1000-fold (Harrington et al., 1992; Moshous et al., 2001). This clearly raises the possibility that there might be some relationship between DNA-PK_{cs} and Artemis. No enzymatic activity has thus far been reported for Artemis.

Here we report that DNA-PK_{cs} and Artemis form a physical complex in which DNA-PK_{cs} efficiently phosphorylates Artemis. We also show that while Artemis alone has 5′ to 3′ exonuclease activity, the Artemis:DNA-PK_{cs} complex endonucleolytically cleaves 5′ and 3′ overhangs and has hairpin-opening activity. Finally, hairpins generated by the RAG complex are efficiently opened by the Artemis:DNA-PK_{cs} complex. This is the first eukaryotic hairpin-opening activity that functions efficiently in magnesium ion-containing buffers. These properties explain the role of Artemis and DNA-PK_{cs} in hairpin opening in V(D)J recombination and its nucleolytic role in nonhomologous DNA end joining.

Results

Artemis and DNA-PK_{cs} Form a Stable Complex In Vitro that Is Independent of DNA Ends

Cells from patients with mutations in the *Artemis* gene have been shown previously to be defective for V(D)J recombination in a manner that is indistinguishable from cells defective for DNA-PK_{cs} (Moshous et al., 2000, 2001). Therefore, we hypothesized that the Artemis protein and DNA-PK_{cs} might be part of a larger complex and involved in similar steps in V(D)J recombination.

To test this hypothesis, human cDNA of *Artemis* was cloned into either GST N-terminal or myc-his C-terminal fusion protein vectors (see Experimental Procedures and Supplementary Data at http://www.cell.com/cgi/content/full/108/6/781/DC1). We began by testing for in vitro interactions between Artemis and DNA-PK_{cs} and between Artemis and Ku using immunobead pull-down experiments. DNA-PK_{cs} was immobilized on protein G sepharose beads using monoclonal antibodies against DNA-PK_{cs}. Purified GST-Artemis was then added. After incubation, the beads were washed stringently to remove any unbound molecules, and the pull-down fraction was analyzed by Western blotting. GST-Artemis associated with DNA-PK_{cs} at 0 and 100 mM KCl (Figure 1A, lanes 5 and 6), but the interaction was unstable at 500 mM KCl (Figure 1A, lane 7). The top portion of the membrane shows that DNA-PK_{cs} is present under all salt conditions on the beads. (Note that while Coomassie staining of the DNA-PK_{cs} shows that the majority of it is full-length (see Figure 1B, lane 1), the residual lower molecular weight fragments transfer much more efficiently than the full-length form in Western blotting, thus explaining the apparent presence of prominent degradation products.)

Because Ku associates with DNA-PK_{cs} on DNA ends to form the DNA-PK holoenzyme, we did the corresponding experiment with immobilized Ku. There was no evidence of interaction between Artemis and Ku (Figure 1A, lanes 9–12). After probing the Western blot with anti-GST antibodies, the bottom portion of the membrane was stripped and reprobed for Ku, which confirmed that Ku was indeed present on the beads under all salt concentrations (data not shown).

Based on these results, we conclude that Artemis and DNA-PK_{cs} can form a stable complex in physiologic ionic strength in the absence of DNA in vitro. Ku and Artemis do not form such a complex. Even in the presence of linear dsDNA, we did not detect interaction between Ku and Artemis by an electrophoretic mobility shift assay (data not shown).

Artemis and DNA-PK_{cs} Form a Stable Complex In Vivo

To test whether Artemis and the 469 kDa DNA-PK_{cs} form a complex in vivo, we transfected an Artemis-myc-His expression plasmid into 293T cells. Then Artemis and any potentially associated protein(s) were immunoprecipitated from transfected cells using anti-myc antibody bound to protein G sepharose beads. DNA-PK_{cs} was

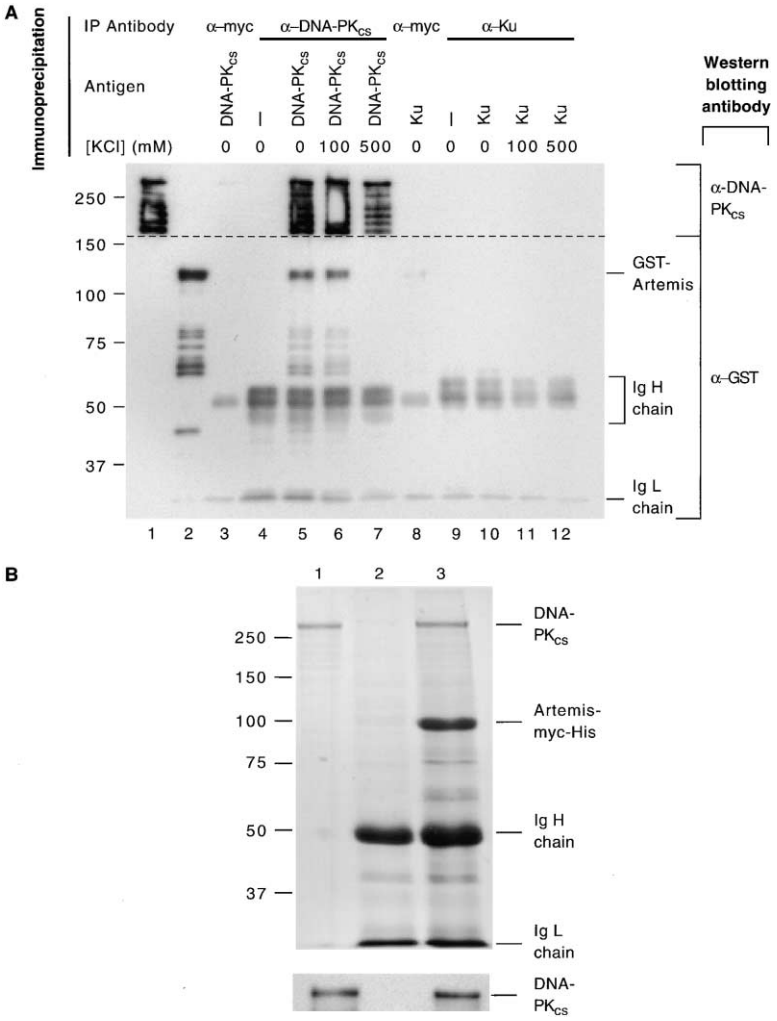

Figure 1. DNA-PK$_{cs}$ Interacts with Artemis

(A) DNA-PK$_{cs}$, but not Ku, interacts with Artemis in vitro. A Western blot analysis of an immunobead pull-down of Artemis is shown. Purified DNA-PK$_{cs}$ and GST-Artemis were loaded in lanes 1 and 2, respectively. DNA-PK$_{cs}$ (lanes 5–7) or Ku (lanes 10–12) were immobilized on antibody-protein G sepharose beads at different concentrations of KCl. As a control, Anti-myc antibody was used in lanes 3 and 8. DNA-PK$_{cs}$ and Ku were excluded from lanes 4 and 9, respectively. After GST-Artemis was added, the beads were washed with the corresponding binding buffer, then analyzed by Western blotting with anti-DNA-PK$_{cs}$ antibodies (portion above the dotted line) and anti-GST antibody (portion below the dotted line). GST-Artemis has an apparent molecular weight of 120 kDa on this 8% SDS-polyacrylamide gel, and the bands of smaller sizes in lane 2 represent C-terminal degradation products of GST-Artemis. Positions of GST-Artemis and immunoglobulin heavy chain and light chain are indicated on the right. Protein molecular weight standards (in kDa) are indicated on the left.

(B) Artemis interacts with DNA-PK$_{cs}$ in vivo. Coomassie staining of immunoprecipitation samples with anti-myc antibody is shown in the upper panel. Purified DNA-PK$_{cs}$ was loaded in lane 1. Cell lysates were subjected to immunoprecipitation with anti-myc antibody, and the immunobeads were loaded in lanes 2 (from transfection with empty vector) and 3 (from transfection with Artemis-myc-His-expressing vector). Protein molecular weight standards are indicated on the left. Positions of DNA-PK$_{cs}$, Artemis-myc-His, and immunoglobulin heavy chain and light chain are indicated on the right. Samples used for the top panel were also subject to Western blotting analysis, and the result is shown in the lower panel. The blot was probed with monoclonal anti-DNA-PK$_{cs}$ antibodies (42–27, 25–4, and 18–2).

coimmunoprecipitated as identified by size on Coomassie-stained gels (Figure 1B, top, lane 3). The identity of DNA-PK$_{cs}$ was confirmed by Western blotting (Figure 1B, bottom). This interaction was stable at 100 mM KCl with or without nonionic detergent, but was unstable at 500 mM KCl (data not shown). The control immunoprecipitation in which the expression vector lacking the Artemis cDNA was transfected showed no detectable DNA-PK$_{cs}$ (Figure 1B, top and bottom, lane 2). These results strongly suggest that Artemis and DNA-PK$_{cs}$ form a stable complex in vivo.

DNA-PK$_{cs}$ Phosphorylates Artemis

Given that Artemis and DNA-PK$_{cs}$ form a complex, we were interested in knowing whether Artemis is a phosphorylation substrate of DNA-PK$_{cs}$. Artemis was indeed a prominent phosphorylation target of DNA-PK$_{cs}$, as illustrated by the DNA-dependent phosphorylation (see Supplemental Figure S2, lanes 5 and 6 at http://www.cell.com/cgi/content/full/108/6/781/DC1). Therefore, DNA-PK$_{cs}$ not only forms a physical complex with Artemis, but also is able to phosphorylate it.

Artemis Is a Single-Strand-Specific Nuclease with a 5′ to 3′ Exonucleolytic Polarity

In the original identification of Artemis, the homology of the N-terminal region of Artemis to SNM1 was described (Moshous et al., 2001). The SNM1 protein and the homologous region of Artemis were predicted to contain β lactamase folds, which were known to function enzymatically in reactions that utilize water molecules as nucleophiles to break covalent bonds. For this reason, our initial characterizations of Artemis alone included testing for nucleolytic activity.

To test this, we performed time course experiments using single-stranded (ss) DNA labeled at its 5′ end using polynucleotide kinase or at its 3′ end using [α-^{32}P]dideoxyadenosine triphosphate (ddATP) and terminal deoxynucleotidyl transferase (TdT). In this nuclease assay, the 5′ radiolabeled ssDNA yielded only a 1 nt product (Figure 2, lanes 2–4). However, a 3′ radiolabeled ssDNA yielded a ladder of products, terminating at 2 nt (Figure 2, lanes 6–7), suggesting that nucleic acid targets must be larger than 2 nt for Artemis to bind and/or cleave. Overall, these results suggest that Artemis pos-

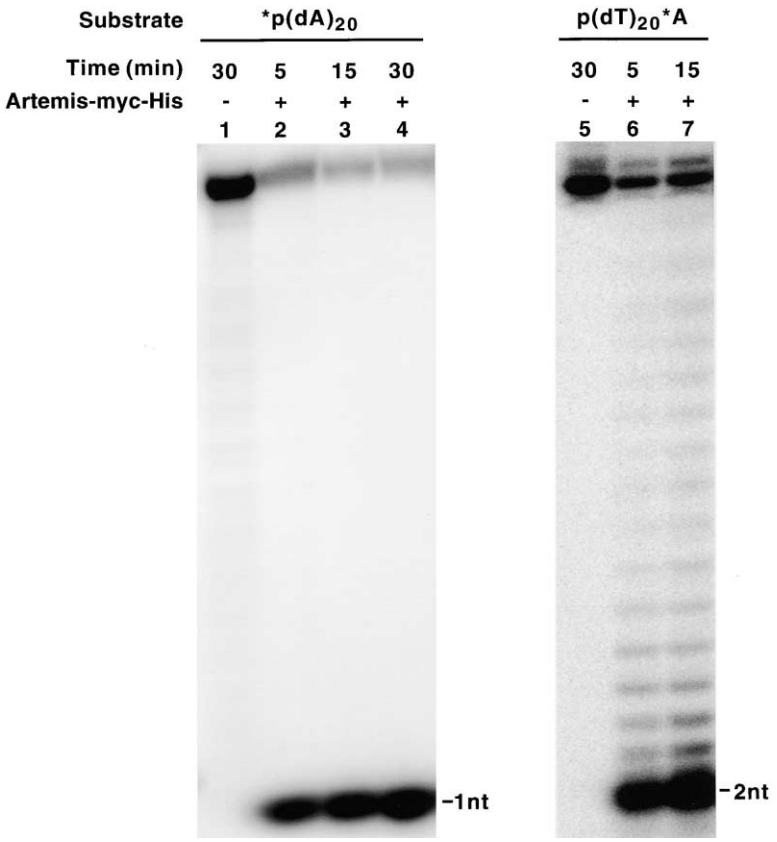

Figure 2. Artemis Is a 5′ to 3′ Single-Strand Exonuclease

Single-stranded poly dA 20-mer was labeled using T4 polynucleotide kinase (T4 PNK) and incubated for the specified times with Artemis-myc-His (lanes 2–4). In lanes 5–7, a poly dT 20-mer was 3′ labeled using terminal deoxynucleotidyl transferase and [α-^{32}P]dideoxyadenosine triphosphate. The 2 nt product size was confirmed by treating the substrate with snake venom phosphodiesterase.

sesses 5′ to 3′ exonuclease activity on ssDNA. If Artemis were a 3′ exonuclease, then initially the 3′ A would be removed and only a mononucleotide product would be observed (Figure 2, lanes 6 and 7). In addition, the 5′ labeled ssDNA would yield a degradation ladder. The 5′ to 3′ single-strand exonuclease activity of Artemis appeared to be processive rather than distributive because there was extensive cleavage of a large fraction of the ss molecules while other molecules in the same population had not been cleaved at all (Figure 2, lanes 6 and 7, and data not shown).

The specificity of Artemis on ssDNA was examined with dsDNA with GC- or AT-rich ends, and DNA with increasing numbers of terminal mismatches (see Supplemental Figure S3 at http://www.cell.com/cgi/content/full/108/6/781/DC1). Artemis showed very limited nucleolytic activity on dsDNA molecules (see Supplemental Figure S3A). This indicates that Artemis is relatively specific for ssDNA with no endonuclease activity on dsDNA. The preference of Artemis for AT-rich ends suggested that breathing at dsDNA ends might account for this. This hypothesis was supported by the fact that the exonucleolytic activity of Artemis increases markedly on substrates with increasing numbers of terminal mismatches (see Supplemental Figure S3B). Altogether, these results indicate that Artemis alone is a 5′ to 3′ single-strand-specific exonuclease. It is also noteworthy that the 5′ exonucleolytic activity is strongly dependent on the presence of a 5′ phosphate and is equivalently active on RNA as on DNA (data not shown). Temperature and ionic strength dependence studies showed that 37°C and 50 mM KCl were optimal (data not shown). Importantly, Artemis was only active as a nuclease in Mg^{2+}-containing buffers and was inactive in corresponding Mn^{2+}- and Zn^{2+}-containing buffers (data not shown).

DNA-PK$_{cs}$ Regulates the Overhang Endonucleolytic Activity of Artemis

We were interested in how Artemis would act on substrates with long 5′ overhangs. Time courses of Artemis action on substrates with long (15 nt poly dT) 5′ overhangs showed that the 5′ mononucleotide was the initial cleavage product, with no intermediate products (Figure 3A, lanes 1–4). Therefore, it appears that Artemis recognizes long 5′ overhangs as ssDNA. A substrate composed of a 21 bp double-stranded portion and a 15 nt poly T 3′ overhang was also tested (Figure 3B), and the products indicated 5′ exonucleolytic cleavage (Figure 3B, lanes 1–4, bottom of gel). (The 5′ exonucleolytic cleavage occurs 2 nt from the 5′ end on some dsDNA substrates [Figure 3B, lanes 2–4], instead of 1 nt, as we observed for purely ssDNA [Figure 2].)

The nucleolytic properties of Artemis alone were important to establish; however, the in vivo protein interaction studies described above indicate that Artemis functions as a complex with DNA-PK$_{cs}$. Therefore, we evaluated the nuclease activity of Artemis along with DNA-PK$_{cs}$. In the presence of DNA-PK$_{cs}$, Artemis showed a very signficant shift in the ratio of cleavage products on DNA with long 5′ overhangs (Figure 3A, lanes 2–4 versus 5–7). With DNA-PK$_{cs}$ present instead of only the

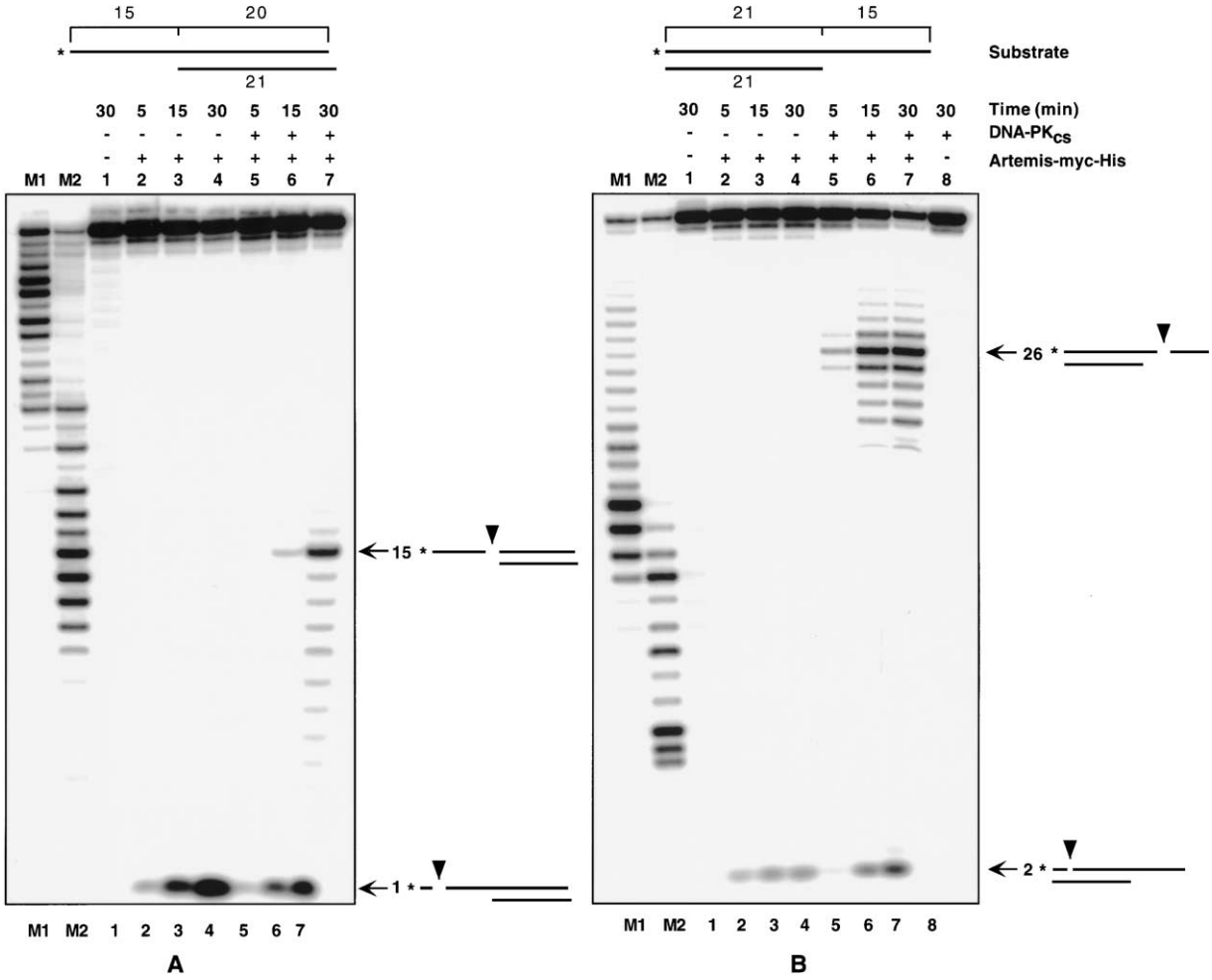

Figure 3. DNA-PK$_{cs}$ Increases the Overhang Endonucleolytic Specificity of Artemis-myc-His

A ds oligonucleotide with a 5′ 15 nucleotide (A) or a 3′ 15 nucleotide (B) (thymidine) overhang was labeled by T4 PNK on the long strand (as indicated by the asterisk) and was used as the substrate. Lanes M1 and M2 contain size standards generated by digesting the top strand of the substrate with Klenow fragment for 30 min and 60 min, respectively. A time course of the degradation of the substrate by Artemis-myc-His alone (lanes 2–4) or Artemis and DNA-PK$_{cs}$ (lanes 5–7) is shown. A control reaction of DNA-PK$_{cs}$ and the substrate is also included (lane 8 in [B]). Sizes of the major products (in nt) are indicated on the right. Diagrams in the right margin are depicted to show the cleavage positions (shown by arrowheads) in the substrate that result in the corresponding degradation products (the bands pointed by arrows).

5′ mononucleotide product, Artemis generated a series of endonucleolytic cleavages internal to the 5′ end, but with a significant predilection for cleavage at the position that yielded a blunt-ended dsDNA product and a labeled 15 nt ssDNA product (Figure 3A, lanes 6 and 7). DNA-PK$_{cs}$ alone had no such activity (data not shown), and Artemis alone only generated the 5′ mononucleotide product as described above (Figure 3A, lanes 2–4). Labeling at the 3′ end of the same strand confirmed these findings (data not shown). Interestingly, at shorter times (Figure 3A, lane 6), predominantly the 5′ mononucleotide and the 15 nt product from the overhang endonucleolytic cleavage reaction were observed.

We also tested long 3′ overhangs for cleavage by Artemis in the presence of DNA-PK$_{cs}$ using the dsDNA substrate with a 15 nt poly T 3′ overhang. DNA-PK$_{cs}$ enabled Artemis to cleave the 3′ overhang (Figure 3B, lanes 1 and 5–7). The cleavage products at early times were predominantly in the single-stranded tail 4–6 nt from the single- to double-strand transition point (Figure 3B, lane 5). At longer times, the distribution of products ranged from cleavage at the single- to double-strand transition point outward along the single-stranded overhang for approximately 10 nt.

These results indicate that DNA-PK$_{cs}$ not only forms a complex with Artemis but also regulates the spectrum of its activities. Because DNA-PK$_{cs}$ binds at single- to double-strand transitions as found at DNA ends, Artemis would necessarily be recruited to these locations because of its association with DNA-PK$_{cs}$. This may permit a very low or undetectable overhang cleavage activity to become a relatively strong one.

DNA-PK$_{cs}$ Confers DNA Hairpin-Opening Activity on Artemis

Because DNA-PK$_{cs}$ mutants are arrested in V(D)J recombination at the hairpin-opening step and because both Artemis and DNA-PK$_{cs}$ mutant mammals have indistin-

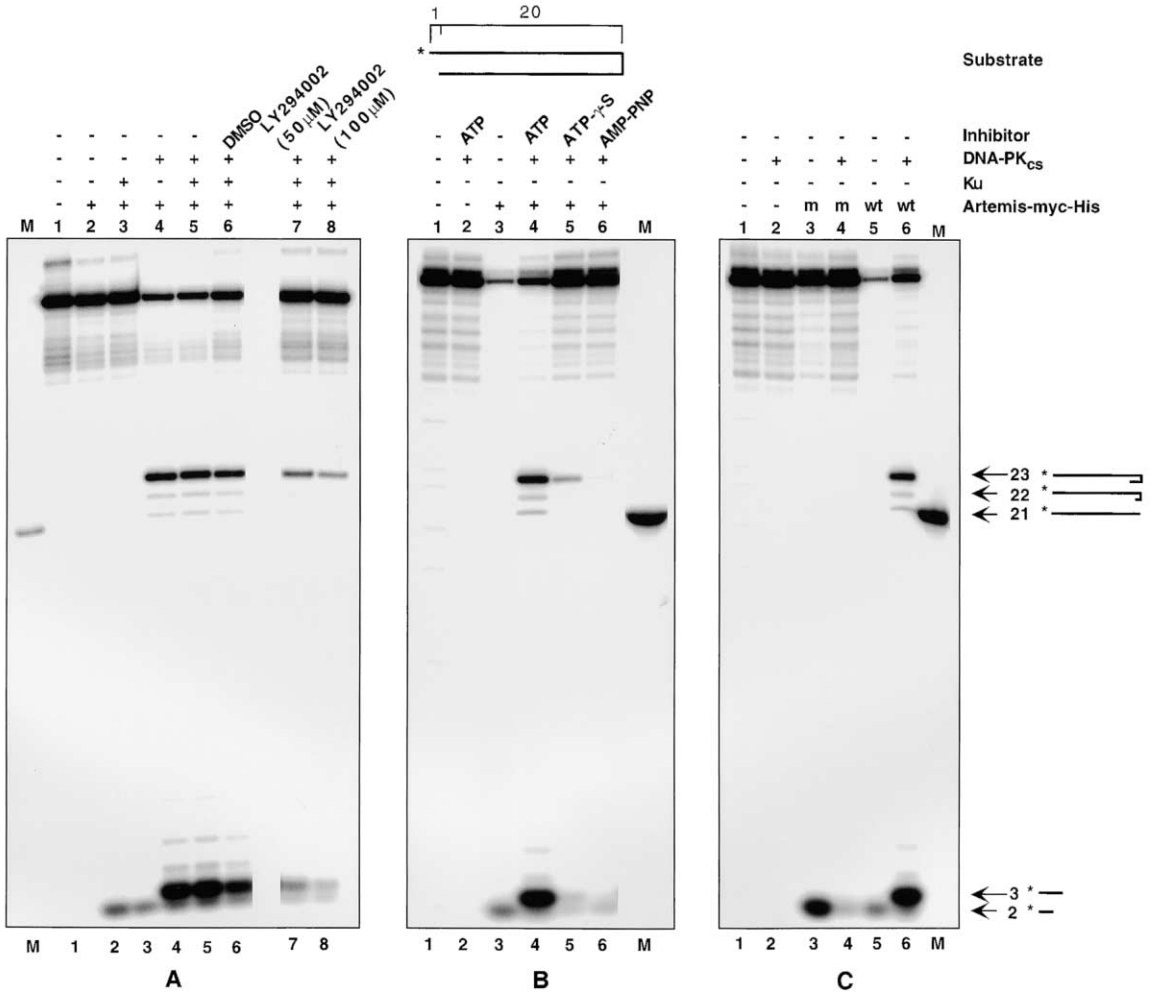

Figure 4. Artemis, But Not an Artemis Point Mutant, Has Hairpin-Opening and Overhang Nuclease Activity in the Presence of DNA-PK$_{cs}$

(A) The hairpin-opening and overhang nuclease activities of Artemis:DNA-PK$_{cs}$ complex are sensitive to the DNA-PK$_{cs}$-inhibitor LY294002. A 20 bp hairpin (D$_{FL16.1}$) with 1 nt 5′ overhang was labeled at the 5′ end with T4 PNK and used as the substrate. In reactions with inhibitors, DNA-PK was either mock treated with DMSO (lane 6) or treated with LY294002 at 50 μM (lane 7) and 100 μM (lane 8) first, then the substrate was added.

(B) The hairpin-opening and overhang nuclease activities of Artemis:DNA-PK$_{cs}$ complex are dependent on ATP. The same substrate was subject to a hairpin-opening assay in presence of 0.25 mM of ATP (lane 4) or 0.25 mM of ATP analogs ATP-γ-S (lane 5) or AMP-PNP (lane 6).

(C) The D$_{FL16.1}$ substrate (same as used in [A] and [B]) was used to test the activities of the D165N mutant (the full-length Artemis used in this paper contains seven upstream amino acids compared to the published sequence [Moshous et al., 2001], resulting in a 692 amino acid protein upon translation) (lanes 3 and 4) and the wild-type Artemis (lanes 5 and 6). Diagrams adjacent to the sizes are depicted to reflect the hairpin-opening positions relative to the substrate. Lane M in (A), (B), and (C) contains an oligonucleotide identical to the fragment 5′ to the hairpin tip (21 nt). Sizes of the major products (in nts) are indicated on the right.

guishable V(D)J recombination phenotypes, it was of interest to determine whether Artemis would act on hairpins. We synthesized a hairpin with the sequence of the murine D$_{FL16.1}$ coding end and tested it as a substrate for Artemis. We observed the expected 5′ to 3′ exonucleolytic activity of Artemis at the nonhairpin (labeled) end of the hairpin DNA substrate, resulting in the generation of a 2 nt product (Figure 4A, lane 2). (Though one might have expected a 1 nt product based on the earlier studies [Figure 2], it appears that the exonucleolytic action of Artemis at DNA ends is somewhat affected by the precise DNA sequence, such that here a 2 nt product results.) No hairpin opening by Artemis alone was detectable (Figure 4A, lane 2). Addition of Ku did not alter the spectrum of Artemis activities (Figure 4A, lane 3). However, the addition of DNA-PK$_{cs}$ substantially shifted the spectrum of nuclease activities of Artemis. With DNA-PK$_{cs}$ present, Artemis efficiently opened about 40% of the hairpins during the time interval (Figure 4A, lanes 4–6). (This is probably an underestimation of the hairpin-opening activity of Artemis, because once the 5′ radiolabel of the substrate is cleaved, the hairpin-opening product becomes invisible on the gel.) This result strongly suggests that DNA-PK$_{cs}$ regulates Artemis activity to include hairpin opening, as well as endonucleolytic cleavage of overhangs.

The position of the hairpin opening varied, but a 3′ overhang was preferentially generated at the opened

end. The predominant hairpin opening was at the +2 position (the phosphodiester bond at the hairpin tip is designated 0, with phosphodiester bonds 3′ to the tip numbered +1, +2, etc., and phosphodiester bonds 5′ to the tip numbered −1, −2, etc.; Figure 4A, lanes 4–8), which corresponds to the 23 nt cleavage product. The DNA-PK$_{cs}$ chemical inhibitor, LY294002, reduces the stimulation (Figure 4A, lanes 7 and 8), while the dimethyl sulfoxide solvent (DMSO) in which LY294002 was dissolved had little effect (Figure 4A, lane 6). To further confirm the importance of DNA-PK$_{cs}$ kinase activity for the hairpin-opening and endonucleolytic activities of Artemis:DNA-PK$_{cs}$ complex, we tested nonhydrolyzable ATP analogs in an Artemis nuclease assay (Figure 4B). As described above, neither DNA-PK$_{cs}$ nor Artemis alone showed any hairpin-opening activity (Figure 4B, lanes 2 and 3). In the presence of ATP, DNA-PK$_{cs}$ was able to confer Artemis efficient hairpin-opening activity (Figure 4B, lane 4). However, this effect of DNA-PK$_{cs}$ was largely suppressed when ATP-γ-S (Figure 4B, lane 5) or AMP-PNP (Figure 4B, lane 6) was used instead of ATP. This indicates the DNA-PK$_{cs}$ kinase activity is critical for the Artemis:DNA-PK$_{cs}$ complex, consistent with the result that Artemis is the substrate of DNA-PK$_{cs}$ in vitro (see Supplemental Figure S2 at http://www.cell.com/cgi/content/full/108/6/781/DC1).

We believe that the nucleolytic properties of the Artemis:DNA-PK$_{cs}$ complex reside within the complex of these two proteins rather than any other protein copurifying with one of them for several reasons. First, the DNA-PK$_{cs}$ preparation is devoid of any nuclease activity (Figure 3B, lane 8, and Figure 4B, lane 2; West et al., 1998; Yaneva et al., 1997). Therefore, the hairpin-opening activity, the overhang nucleolytic activity, and the 5′ to 3′ exonuclease activities are not the result of a contaminating nuclease from the DNA-PK$_{cs}$ preparation. Second, we have identified a SCID patient with a single homozygous point mutation of *Artemis* in the conserved SNM1 domain, and the phenotype of this patient is indistinguishable from those with null mutations of Artemis (U.P. and K.S., unpublished). Third, a point mutant of Artemis lacks any hairpin-opening activity (Figure 4C). The D165N point mutant of Artemis was cloned into the same expression vector and purified along with the wild-type Artemis protein. However, while still having the 5′ to 3′ exonuclease activity, this point mutant was completely devoid of hairpin-opening activity in the presence of DNA-PK$_{cs}$ (Figure 4C, lane 4), similar to the GST-tagged Artemis (see below). These observations strongly support the view that the nucleolytic properties described here reside within the Artemis moiety of the Artemis:DNA-PK$_{cs}$ complex.

DNA-PK$_{cs}$ Regulation of Artemis Is ATP Dependent and Requires the Physical Presence of DNA-PK$_{cs}$

Based on the hypothesis that DNA-PK$_{cs}$ can affect hairpin opening by phosphorylating the protein with hairpin-opening activity, we tested whether phosphorylation of Artemis by DNA-PK$_{cs}$ is necessary to confer hairpin-opening activity on Artemis. A hairpin with a 6 nt 5′ overhang and an entirely GC-hairpin end was used. Artemis alone cleaved the hairpin only at the 5′ overhang (nonhairpin end; Figure 5, lane 2). The Artemis:DNA-PK$_{cs}$ complex opened this hairpin 3′ to the tip at the +1 and +2 positions (Figure 5, lane 5), similar to the positions of hairpin opening of the D$_{FL16.1}$ hairpin as described above. The hairpin opening in Figure 5, lane 5, while present, was clearly less abundant than that seen for the D$_{FL16.1}$ hairpin (Figure 4A, lane 4), even though the 5′ exonuclease and overhang endonuclease action was equally strong. This may be due to the inefficiency of cleavage of the GC-hairpin end. Hence, the sequence of the hairpin may affect the efficiency of hairpin opening.

The hairpin opening and the overhang cleavage were increased in the presence of ATP relative to the level when ADP was present (Figure 5, lane 3 versus 5). A lower level of endonucleolytic activity both on hairpins and 5′ ends was observed in the presence of ADP, but this may be attributable to low levels of contaminating ATP that were present in ADP (Figure 5, lane 3). Therefore, ATP is important for the regulation of Artemis by DNA-PK$_{cs}$, consistent with the finding above that ATP-γ-S and AMP-PNP were unable to replace ATP in the hairpin-opening assay of the Artemis:DNA-PK$_{cs}$ complex. (Figure 4B).

The hairpin opening and the overhang endonucleolytic cleavage were both stimulated by addition of 35 bp dsDNA (Figure 5, lane 4 versus 5). This is consistent with the dsDNA end stimulation of kinase activity of DNA-PK$_{cs}$. The equilibrium binding affinity of DNA-PK$_{cs}$ for dsDNA is approximately 10^{-9} M (West et al., 1998), and the additional dsDNA permits a higher occupancy and, hence, stimulation of DNA-PK$_{cs}$. Interestingly, although Ku increases the affinity of DNA-PK$_{cs}$ to an end, the presence of Ku did not affect the ability of DNA-PK$_{cs}$ to regulate Artemis (Figure 5, lane 6). Neither Ku nor DNA-PK$_{cs}$ showed any nuclease activity on this (or other) substrate (data not shown).

Based on these studies, we knew that Artemis phosphorylation by DNA-PK$_{cs}$ was necessary, but is it sufficient? To test the possibility that Artemis requires not only phosphorylation by DNA-PK$_{cs}$ but also continued physical complex formation with DNA-PK$_{cs}$, we treated bead-immobilized Artemis with DNA-PK$_{cs}$ first and then used the extensively washed beads (presumably containing immobilized and phosphorylated Artemis, devoid of any DNA-PK$_{cs}$) for the nuclease assay. We found that Artemis nuclease activity was equivalent to that of unphosphorylated Artemis, including failure to endonucleolytically open hairpins (Figure 5, lanes 8–11). Hence, the hairpin-opening activity is dependent not only on the phosphorylation but also the physical presence of DNA-PK$_{cs}$. That is, the hairpin-opening activity is strictly a property of the Artemis:DNA-PK$_{cs}$ complex, not of Artemis alone and not of DNA-PK$_{cs}$ alone.

The action of Artemis at the 6 nt 5′ overhang of the hairpin was also altered by the presence and kinase activity of DNA-PK$_{cs}$. Artemis alone removed only 5′ mononucleotides (Figure 5, lane 2). Artemis:DNA-PK$_{cs}$ preferentially removed 5 and 6 nt products in the presence of ATP (Figure 5, lanes 5 and 6). This is consistent with the overhang endonucleolytic cleavage activity described above (Figure 3A), and given the length of this 5′ overhang, the 5 and 6 nt cleavage products are fully expected. Furthermore, the prephosphorylated Artemis only generated mononucleotide products, instead of the

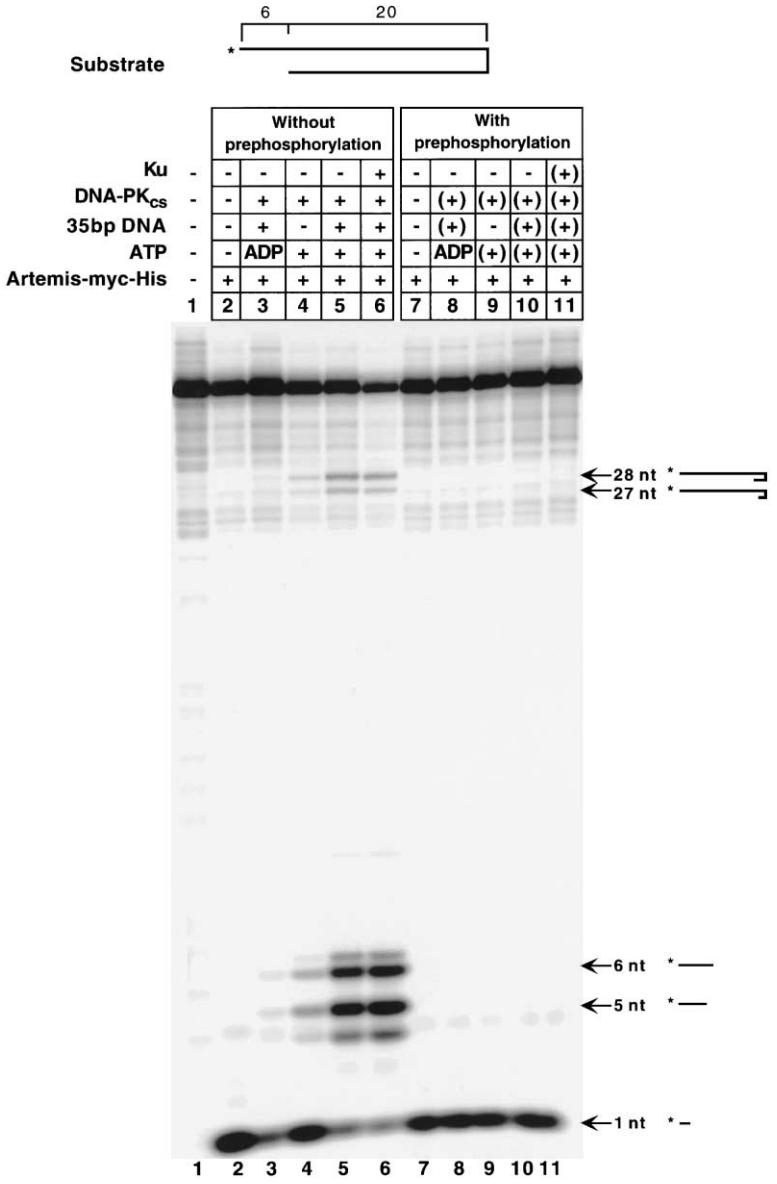

Figure 5. Both the Activity and Presence of DNA-PK$_{cs}$ Are Required for the Hairpin-Opening and Overhang Nuclease Activities of Artemis

A 20 bp artificial hairpin with 6 nt 5′ overhang was labeled by T4 PNK and used as the substrate. Reactions without prephosphorylation (lanes 2–6) were carried out such that the reagents indicated were mixed with the substrate at the same time. However, in reactions with prephosphorylation (lanes 7–11), the reagents indicated were mixed with Artemis-myc-His immunobeads first and incubated to allow the phosphorylation of Artemis; then DNA-PK$_{cs}$ and other reagents were washed away from the immunobeads. Finally, the nuclease assay was performed with the treated beads (but without DNA-PK$_{cs}$, etc.) and the substrate. The + symbols on top of these lanes (7–11) indicate that these reagents were only present in the prephosphorylation of Artemis and not in the nuclease reactions. Sizes of the major products are indicated on the right. Diagrams adjacent to the sizes are depicted to reflect the hairpin-opening positions relative to the substrate.

5 and 6 nt overhang cleavage products (Figure 5, lanes 10 and 11), indicating that the presence of DNA-PK$_{cs}$ is also important for stimulating the overhang endonuclease activity of Artemis.

The GST-Artemis has identical 5′ to 3′ exonucleolytic and overhang endonuclease properties to Artemis-myc-His, except that GST-Artemis is distinctly weaker in activity (~10-fold) and GST-Artemis fails to open hairpins at any detectable level, even though it is able to form a complex with DNA-PK$_{cs}$ (Figure 1A). This raises the possibility that the N-terminal region of Artemis is important, perhaps for conformational reasons, for all of the nucleolytic activities of Artemis. This is consistent with the fact that the SNM1 homologous region of Artemis resides in the N-terminal region (Moshous et al., 2001).

The Artemis:DNA-PK$_{cs}$ Complex Can Open RAG Complex-Generated Hairpins

We were interested in testing the hypothesis that the Artemis:DNA-PK$_{cs}$ complex could open hairpins generated by the RAG complex (RAG-1, RAG-2, and HMG1). We carried out this experiment in three different configurations. In one configuration, the DNA was phenol/chloroform extracted after the RAG complex treatment, before exposure of any RAG-generated hairpins to the Artemis:DNA-PK$_{cs}$ complex. In a second configuration, no organic extraction was included, but the Artemis:DNA-PK$_{cs}$ complex was added after the RAG complex had generated hairpins. In the third configuration, the RAG complex and the Artemis:DNA-PK$_{cs}$ complex were added simultaneously. The starting DNA substrate for all three configurations was a radiolabeled 12-RSS substrate accompanied by an unlabeled 23-RSS substrate; this permits the reaction to proceed according to the 12/23 rule, which is essential for efficient hairpin formation in V(D)J recombination in vivo and in vitro. Hairpin formation by the RAG complex was efficient in all of the reactions (Figure 6, lanes 2–4, 6–8, and 10–12). Hairpin opening was also detectable for all three experimental configurations (Figure 6, lanes 4, 8, and 12), indi-

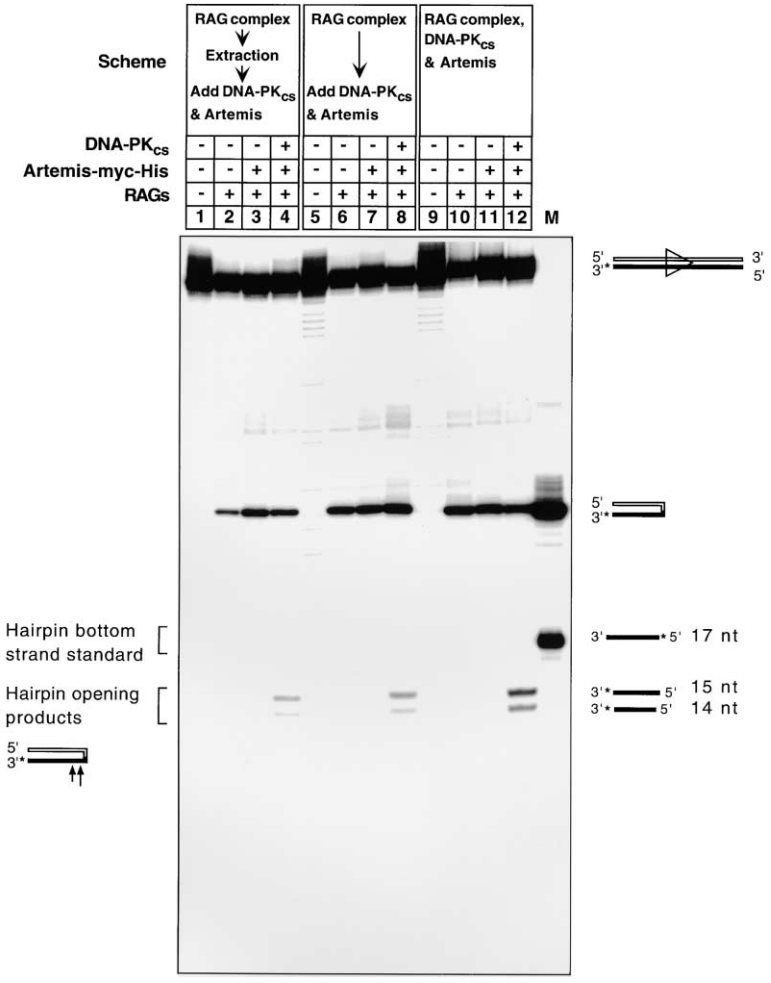

Figure 6. The Artemis:DNA-PK$_{cs}$ Complex Can Open RAG-Generated Hairpins

A ds oligonucleotide containing a 12-RSS (open triangle) was labeled at the 3′ end on the bottom strand with Klenow fragment, as indicated by the asterisk. An unlabeled 23-RSS containing ds oligonucleotide was present during the reaction in addition to the 12-RSS ds oligonucleotide to allow efficient hairpin formation by RAGs according to the 12/23 rule. The reaction schemes are shown as brief flow charts. In reactions with multiple steps, substrates were either incubated with the RAG complex first, followed by phenol/chloroform extraction (lanes 1–4), or no organic extraction was included (lanes 5–8), and then Artemis-myc-His and DNA-PK$_{cs}$ were added. In one-step reactions (lanes 9–12), all proteins were added to the reaction at the start of the incubation. Synthetic oligonucleotides identical to the RAG-generated hairpin and the hairpin tip opening product were coelectrophoresed in lane M. Sizes of the major products are indicated on the right. The diagrams for the substrate and the hairpin are shown as base paired to emphasize the native structures. For the clarity of presentation, the top (unlabeled) strand of the substrate and the fragment of the hairpin that originates from the top strand are depicted as open bars.

cating that the RAG postcleavage complex does not block the Artemis:DNA-PK$_{cs}$ complex from opening the hairpins efficiently. The size of the hairpin-opening products (Figure 6, lanes 4, 8, and 12) is consistent with the fact that Artemis opens hairpins 3′ to the tip (Figures 4 and 5). This is the first efficient opening of RAG-generated hairpins by any vertebrate nuclease in Mg^{2+}-containing solutions.

Discussion

The findings here provide insights into several previously unanswered questions in V(D)J recombination and in NHEJ. First, what is the hairpin-opening activity for V(D)J recombination? Second, what is the physiologic phosphorylation target of DNA-PK$_{cs}$ in the context of V(D)J recombination? Third, why does the absence of DNA-PK$_{cs}$ result in failure to open the hairpinned coding ends, despite the fact that DNA-PK$_{cs}$ has no nuclease activity of its own, nor can DNA-PK$_{cs}$ confer efficient hairpin-opening activity on the RAG complex? Fourth, if Artemis is the hairpin-opening activity, what is its role in general NHEJ, where dsDNA ends, rather than hairpins, must be processed?

Here we have described protein complex formation between Artemis and DNA-PK$_{cs}$ in the absence of DNA or DNA termini. Artemis alone is a 5′ to 3′ single-strand exonuclease. The Artemis:DNA-PK$_{cs}$ complex is an overhang endonuclease and a hairpin endonuclease. The hairpin opening and overhang endonuclease activities of Artemis require the presence and phosphorylation by DNA-PK$_{cs}$. The Artemis:DNA-PK$_{cs}$ complex is able to open hairpins that are generated by the RAG complex in Mg^{2+}-containing buffers and without removal of the RAG complex. These findings provide compelling evidence that the hairpin opening in V(D)J recombination and overhang processing in NHEJ are conducted by the Artemis:DNA-PK$_{cs}$ complex (see Supplemental Figure S1 at http://www.cell.com/cgi/content/full/108/6/781/DC1).

Artemis:DNA-PK$_{cs}$ as a Protein Complex

Artemis and DNA-PK$_{cs}$ form a complex that is stable under physiologic ionic strength and does not rely on DNA termini or Ku for stability. This raises the possibility that this is the functional state of Artemis inside the cell, given that DNA-PK$_{cs}$ is a relatively abundant nuclear protein and the level of Artemis expression is low (Anderson and Carter, 1996; Moshous et al., 2001). This would be consistent with the phenotypic similarity concerning X-ray sensitivity, as well as signal joint formation but failure of coding joint formation in Artemis and DNA-PK$_{cs}$ mutants.

Furthermore, we show that DNA-PK$_{cs}$ efficiently phosphorylates Artemis upon complex formation and that this activity is dependent on DNA ends. These results imply that the Artemis:DNA-PK$_{cs}$ nuclease complex would be ideally responsive to pathologic dsDNA breaks.

Artemis:DNA-PK$_{cs}$ as a Structure-Specific Nuclease

Though Artemis alone has 5′ to 3′ exonuclease activity, it is likely that Artemis and DNA-PK$_{cs}$ function as a complex. Since DNA-PK$_{cs}$ alone did not show nuclease activities, the nucleolytic active site probably resides in Artemis, and the failure of a point mutant of Artemis to open hairpins (Figure 4C) strongly supports this argument. The fact that the regulation of Artemis endonucleolytic activity by Artemis:DNA-PK$_{cs}$ is ATP-dependent indicates that the kinase activity of DNA-PK$_{cs}$ is necessary. Interestingly, pretreatment of Artemis with DNA-PK$_{cs}$ and ATP is not sufficient to confer overhang cleavage and hairpin-opening activity on Artemis. DNA-PK$_{cs}$ must remain present, even after the phosphorylation, for efficient hairpin opening. It remains to be determined whether the key protein phosphorylation events within the Artemis:DNA-PK$_{cs}$ complex are DNA-PK$_{cs}$ phosphorylation of itself, of Artemis, or both.

For general NHEJ, the overhang endonucleolytic activity of Artemis is clearly more relevant than hairpin opening. Apparently, this aspect of DNA end processing is sufficiently important that cells deficient for it are X-ray sensitive. This activity is insensitive to the 2′ OH of the sugar (because RNA is also cleaved) and largely insensitive to the identity of the base; hence, it is a general structure-specific overhang nuclease.

The Distribution of Products Resulting from the Hairpin Opening Is Very Similar to Those Generated In Vivo at the Corresponding Chromosomal Loci

It is interesting to examine the locations on the hairpin at which Artemis:DNA-PK$_{cs}$ hydrolyzes the phosphodiester bond. We studied the D$_{FL16.1}$ and J$_{H1}$ coding end hairpins as free and RAG-generated hairpins (Figures 4A–4C and 6, and data not shown). In both cases, the pattern of hairpin opening corresponds to opened hairpins generated in the chromosomes of primary thymic T cells and in lymphoid cell lines as determined by Schlissel (1998). Specifically, our study and the Schlissel study describe preferential (but not exclusive) hairpin opening 3′ to the hairpin tip. This correspondence suggests that the Artemis:DNA-PK$_{cs}$ hairpin-opening activity in vitro functions very similarly to the hairpin-opening activity observed in vivo.

When hairpins are opened at positions other than the precise tip, an inverted repeat is generated at the resulting overhang. Such inverted repeats were described initially in V(D)J recombination coding joints in chickens (McCormack et al., 1989) and were named P (palindromic) nucleotides. They were subsequently identified in V(D)J recombination junctions in all vertebrates. P nucleotides were speculated to arise as a result of opening of hairpin intermediates at nontip positions (Lieber, 1991). This origin of P nucleotides was firmly established by the identification of hairpin intermediates in DNA-PK$_{cs}$-deficient and, subsequently, Ku-deficient cells (Roth et al., 1992; Zhu et al., 1996). The preferential cleavage of DNA hairpins by the Artemis:DNA-PK$_{cs}$ complex provides an enzymatic basis for completing the understanding of P nucleotide formation.

Junctional diversification at coding joints in V(D)J recombination consists not only of P nucleotide formation but also nucleotide loss and TdT-dependent additions (Gauss and Lieber, 1996; Lewis, 1994; Lieber, 1991). In fact, most V(D)J recombination junctions do not show any P nucleotides at their coding joints, but rather show nucleotide loss from both coding ends (Gellert, 1997; Lewis, 1994; Lieber, 1998). This may be the result of the endonucleolytic cleavage activity of the Artemis:DNA-PK$_{cs}$ complex. Thus, the Artemis:DNA-PK$_{cs}$ complex may directly participate in the junctional diversification.

A Unifying Hypothesis for the Endonucleolytic Structural Specificities of Artemis:DNA-PK$_{cs}$ for DNA Hairpin Opening and for Single-Stranded Overhangs

The positional preferences for the 5′ overhang, 3′ overhang, and hairpin endonucleolytic activities of Artemis:DNA-PK$_{cs}$ may have a unifying explanation (Figure 7). On 5′ overhangs (Figure 7A), the endonucleolytic cleavage preference is directly at the single- to double-strand transition (Figure 3A). On 3′ overhangs (Figure 7B), the endonucleolytic cleavage preference is displaced ~4 nt into the single-stranded region (Figure 3B). Hence, it appears that Artemis:DNA-PK$_{cs}$ recognizes 4 nt of ssDNA (nearest to a double-strand transition) in an orientation-dependent manner (Figures 7A and 7B, thick arrows), and it preferentially cleaves at the 3′ side of that 4 nt ssDNA region.

Nuclear magnetic resonance data suggests that DNA hairpins have unpaired bases near the tip, resulting in a 2–4 nt single-stranded loop at the tip (Figure 7C; Blommers et al., 1989; Howard et al., 1991; Raghunathan et al., 1991). In this study of the hairpin substrates, the endonucleolytic preference is ~2 nt 3′ to the hairpin tip (Figures 4A–4C, 5, and 6). If one considers the hairpin as a single-stranded 5′ extension of the bottom strand (Figure 7D), then the overhang studies (Figures 3A and 5) would predict preferential cleavage 3′ of the fourth nucleotide in a 4 nt hairpin loop. This is the region where we see the hairpin-opening preference. Likewise, if one regards the hairpin as a 3′ extension of the top strand (Figure 7E), then one would predict cleavage 3′ of the four single-stranded nucleotides at the hairpin end, based on the overhang studies (Figure 3B). This, again, is the same preferred position as observed in the hairpin-opening studies (Figures 4A–4C, 5, and 6). Therefore, the 5′ and 3′ overhang studies both predict the same positional preference in the hairpin, and that is where the observed preferential cleavage occurs (Figures 7C–7E). This suggests that the Artemis moiety of the Artemis:DNA-PK$_{cs}$ complex recognizes approximately a 4 nt single-stranded region of the hairpin tip and cleaves 3′ to that 4 nt region (Figure 7C). We note the obvious variation in cleavage around these preferential sites. Moreover, the binding of Ku and other proteins may result in greater lengths of hairpin melting, and this might permit Artemis:DNA-PK$_{cs}$ to cleave more internally, thereby causing deletions deeper into the coding end. The variation in coding end nucleotide loss is known to have clear evolutionary utility for V(D)J recombination.

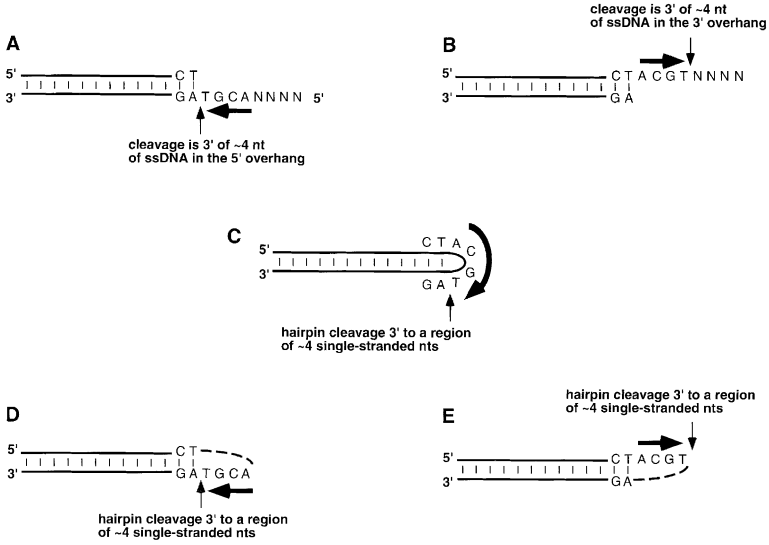

Figure 7. A Model to Unify the Endonucleolytic Properties of the Artemis:DNA-PK$_{cs}$ Complex

(A and B) Schematic structures of dsDNA with a 5′ and a 3′ overhang, respectively. Thin arrows in (A) and (B) mark the major cleavage sites observed in Figures 3A and 3B on similar DNA structures, respectively. N represents any nucleotide in the overhangs.

(C) Hairpin with $D_{FL16.1}$ coding end sequence (substrate for Figures 4A–4C, only the terminal 8 nt shown) is depicted to show the major cleavage position (2 nt 3′ to the hairpin tip or +2 position, marked by the thin arrow) by Artemis:DNA-PK$_{cs}$ complex.

(D and E) The same hairpin substrate as shown in (C) but with emphasis on the structural similarity to dsDNA with a 5′ and a 3′ overhang, respectively. Dashed lines in (D) and (E) represent the artificially stretched phosphodiester bonds at the −2 and +2 positions, respectively. In all panels, the thick arrow depicts the hypothesized recognition region by Artemis, which seems to bind near the junction of single- and double-strand DNA and have an active site near the head of the arrow. Thus, the seemingly diverse endonucleolytic activities of Artemis:DNA-PK$_{cs}$ complex might reside in one active domain.

The exonucleolytic activity of Artemis alone may be regarded as unregulated, and clearly this activity is insufficient for general NHEJ (and for V(D)J recombination) because DNA-PK$_{cs}$ mutants are sensitive to ionizing radiation (Hendrickson et al., 1991). The orientational polarity of Artemis:DNA-PK$_{cs}$ on 5′ and 3′ overhangs may be a reflection of the polarity of Artemis alone as a 5′ to 3′ exonuclease. Further studies will be needed to test the various aspects of this model.

Upon complex formation with and phosphorylation by DNA-PK$_{cs}$, the spectrum of activities of Artemis is shifted from exonucleolytic to endonucleolytic. This is an interesting but not unique phenomenon. There are other examples of nucleases that have both exo- and endonuclease activity. *E. coli* RecBCD, although an endonuclease, acts exonucleolytically while translocating on its DNA substrate as a helicase (Kowalczykowski and Eggleston, 1994). In eukaryotes, FEN-1 has also been shown to have both exo- and endonuclease activity. Relevant to the Artemis mutant described here, it has been reported that some mutations in FEN-1 affect the exonucleolytic activity but not the endonucleolytic activity and vice versa (Xie et al., 2001), despite the fact that there is only one nucleolytic active site in FEN-1 (Lieber, 1997; Shen et al., 1996).

The Evolution of the Artemis:DNA-PK$_{cs}$ Complex within the NHEJ Pathway

Though Ku70, Ku86, DNA ligase IV, and XRCC4 exist in all eukaryotes, including yeast and plants (Lieber, 1999; West et al., 2000), DNA-PK$_{cs}$ and Artemis are thus far only detectable in vertebrates (Moshous et al., 2001). What is distinctive about vertebrates that required the evolutionary introduction of two proteins to the NHEJ pathway that did not exist elsewhere among any other eukaryotes? Clearly, the use of a transpositional excision mechanism that generates hairpins, namely, V(D)J recombination, is one obvious distinction of vertebrates.

Based on this, there appears to be no need for a hairpin-opening activity in the absence of hairpin or hairpin-like DNA structures in nonvertebrate eukaryotes. Mre11, together with Rad50 and Xrs2, have been proposed as candidates for open hairpinning in vivo (Paull and Gellert, 1998). However, the biochemical support for such an in vivo role of Mre11 is compromised by the fact that no hairpin opening has been demonstrated under physiologic divalent salt conditions (Paul, 1999; Paull and Gellert, 1998, 1999). Rather, Mre11 opening of hairpins has only been achieved in manganese buffers, which can distort the physiologic spectrum of nuclease activities. Moreover, Nbs1 (Xrs2) mutant patients and cells from them appear to have normal V(D)J recombination (Harfst et al., 2000; Yeo et al., 2000). In marked contrast, patients with two mutant Artemis alleles cannot form coding joints, and thus have no mature B or T cells; this indicates that Mre11 is unable to provide any backup function for hairpin opening in vertebrates when Artemis is absent (Moshous et al., 2000, 2001). In yeast, where homologs of Artemis and DNA-PK$_{cs}$ do not appear to exist, artificial cruciforms require the Rad50/Xrs2/Mre11 complex for resolution (Lobachev et al., 2002). Though cruciforms have hairpins within their structure, it is not clear from that study that Mre11 is actually cleaving those hairpins, or whether the Rad50/Xrs2/Mre11 complex plays another role in the resolution of such structures.

The role of the Artemis:DNA-PK$_{cs}$ complex as an overhang nuclease in NHEJ may be served by other proteins (such as FEN-1 [Rad27 in *S. cerevisiae*]) (Wu et al., 1999). Due to the structural resemblance of overhangs to hairpin structures (Figure 7), the evolution of the Artemis:DNA-PK$_{cs}$ complex may have made other overhang nucleases in NHEJ unnecessary in vertebrates. The radiation sensitivity of Artemis and of DNA-PK$_{cs}$ mutants (Hendrickson et al., 1991; Nicolas et al., 1998) suggests the 5′ and 3′ overhang processing by this complex cannot be accomplished by any of the other nucleases in the cell.

Experimental Procedures

Construction of GST-Artemis- and Artemis-myc-His-Expressing Plasmids

Full-length human Artemis cDNA was amplified by recombinant Pfu DNA polymerase, and a GST-Artemis-expressing plasmid and an Artemis-myc-His-expressing plasmid were generated as described in full detail in the Supplemental Data at http://www.cell.com/cgi/content/full/108/6/781/DC1.

Protein Purification

Soluble GST-Artemis, immunobead bound Artemis-myc-His, native DNA-PK_{cs}, and recombinant Ku were purified as described in full detail (see Supplemental Data at http://www.cell.com/cgi/content/full/108/6/781/DC1) and as described previously for the latter two proteins (Ma and Lieber, 2001, 2002; West et al., 1998; Yaneva et al., 1997).

In Vitro Immunobead Pull-Down Assay

Immunobead pull-down assays were done as described previously (Yaneva et al., 1997) and as described in detail in the Supplemental Data at http://www.cell.com/cgi/content/full/108/6/781/DC1.

Immunoprecipitation of DNA-PK_{cs} from Artemis-Transfected Cells

293T cells transfected with empty vector or Artemis-myc-His-expressing plasmid were harvested, washed in 1 × PBS, and then resuspended in 25 mM HEPES (pH 7.4), 150 mM KCl, 10 mM $MgCl_2$, 10% glycerol, and 2 mM DTT supplemented with protease inhibitors (as described in the Supplemental Data at http://www.cell.com/cgi/content/full/108/6/781/DC1). Cells were lysed by sonication and centrifuged as above. Anti-myc antibody and protein G sepharose were added to the cell lysates, and binding was allowed to proceed for 12–16 hr. After being washed extensively in the same buffer, the immunobeads were denatured in sample loading buffer, fractionated on an 8% SDS-PAGE, and then either stained with Coomassie blue or analyzed by Western blotting with anti-DNA-PK_{cs} antibodies.

Oligonucleotides

See Supplemental Data at http://www.cell.com/cgi/content/full/108/6/781/DC1.

In Vitro Nuclease Assays

Nuclease assays without RAGs were carried out in a total volume of 10 μl with a buffer composition of 25 mM Tris (pH 8.0), 10–50 mM NaCl or KCl, 10 mM $MgCl_2$, 1 mM DTT, and 50 ng/μl of BSA unless otherwise specified. To the buffer mixture, Artemis was added to 2.75 pmol, and DNA-PK_{cs} and Ku were added to 1.25 pmol each. Where DNA-PK_{cs} was used, 0.25 mM of ATP (or ADP, ATP-γ-S, AMP-PNP) and 0.5 μM of 35 bp DNA were included. Reactions were incubated at 37°C for 30 min. All additional details are in the Supplemental Data at http://www.cell.com/cgi/content/full/108/6/781/DC1.

Acknowledgments

The authors wish to thank members of the Lieber and Schwarz laboratories for helpful comments throughout the course of the work. The authors thank Dr. Kefei Yu for experimental contributions during the early phase of the work. The authors thank Dr. Chih-Lin Hsieh, Dr. Frederic Chedin, and Zarir E. Karanjawala for comments on the manuscript. This work was supported by National Institutes of Health grants to M.R.L. and a P01 from the National Institute of Aging. M.R.L. is the Rita & Edward Polusky Basic Cancer Research Professor and thanks Rita and Ed Polusky for their support.

Received: December 17, 2001
Revised: February 20, 2002
Published online: March 1, 2002

References

Agrawal, A., and Schatz, D.G. (1997). RAG1 and RAG2 form a stable postcleavage synaptic complex with DNA containing signal ends in V(D)J recombination. Cell *89*, 43–53.

Anderson, C.W., and Carter, T.H. (1996). The DNA-activated protein kinase-DNA-PK. In Molecular Analysis of DNA Rearrangements in the Immune System, R. Jessberger and M.R. Lieber, eds. (Heidelberg: Springer-Verlag), pp. 91–112.

Barnes, D.E., Stamp, G., Rosewell, I., Denzel, A., and Lindahl, T. (1998). Targeted disruption of the gene encoding DNA ligase IV leads to lethality in embryonic tissues. Curr. Biol. *8*, 1395–1398.

Besmer, E., Mansilla-Soto, J., Cassard, S., Sawchuk, D.J., Brown, G., Sadofsky, M., Lewis, S.M., Nussenzweig, M.C., and Cortes, P. (1998). Hairpin coding end opening is mediated by RAG1 and RAG2 proteins. Mol. Cell *2*, 817–828.

Blommers, M.J., Walters, J.A., Haasnoot, C.A., Aelen, J.M., van der Marel, G.A., van Boom, J.H., and Hilbers, C.W. (1989). Effects of base sequence on the loop folding in DNA hairpins. Biochemistry *28*, 7491–7498.

Bosma, M.J., and Carroll, A.M. (1991). The SCID mouse mutant: definition, characterization, and potential uses. Annu. Rev. Immunol. *9*, 323–350.

Chiu, C.Y., Cary, R.B., Chen, D.J., Peterson, S.R., and Stewart, P.L. (1998). Cryo-EM imaging of the catalytic subunit of the DNA-dependent protein kinase. J. Mol. Biol. *284*, 1075–1081.

Dronkert, M.L.G., de Wit, J., Boeve, M., Vasconcelos, M.L., van Steeg, H., Tan, T.L., Hoeijmakers, J.H., and Kanaar, R. (2000). Disruption of mouse SNM1 causes increased sensitivity to the DNA interstrand cross-linking agent mitomycin C. Mol. Cell. Biol. *20*, 4553–4561.

Fugmann, S.D., Lee, A.I., Shockett, P.E., Villey, I.J., and Schatz, D.G. (2000). The RAG proteins and V(D)J recombination: complexes, ends, and transposition. Annu. Rev. Immunol. *18*, 495–527.

Gao, Y., Sun, Y., Frank, K.M., Dikkes, P., Fujiwara, Y., Seidl, K.J., Sekiguchi, J.M., Rathbun, G.A., Swat, W., Wang, J., et al. (1998). A critical role for DNA end-joining proteins in both lymphogenesis and neurogenesis. Cell *95*, 891–902.

Gauss, G.H., and Lieber, M.R. (1996). Mechanistic constraints on diversity in human V(D)J recombination. Mol. Cell. Biol. *16*, 258–269.

Gellert, M. (1997). Recent advances in understanding V(D)J recombination. Adv. Immunol. *64*, 39–64.

Grawunder, U., Wilm, M., Wu, X., Kulesza, P., Wilson, T.E., Mann, M., and Lieber, M.R. (1997). Activity of DNA ligase IV stimulated by complex formation with XRCC4 protein in mammalian cells. Nature *388*, 492–495.

Grawunder, U., West, R.B., and Lieber, M.R. (1998a). Antigen receptor gene rearrangement. Curr. Opin. Immunol. *10*, 172–180.

Grawunder, U., Zimmer, D., Fugmann, S., Schwarz, K., and Lieber, M.R. (1998b). DNA ligase IV is essential for V(D)J recombination and DNA double-strand break repair in human precursor lymphocytes. Mol. Cell *2*, 477–484.

Hammarsten, O., and Chu, G. (1998). DNA-dependent protein kinase: DNA binding and activation in the absence of Ku. Proc. Natl. Acad. Sci. USA *95*, 525–530.

Harfst, E., Cooper, S., Neubauer, S., Distel, L., and Grawunder, U. (2000). Normal V(D)J recombination in cells from patients with Nijmegen breakage syndrome. Mol. Immunol. *37*, 915–929.

Harrington, J., Hsieh, C.-L., Gerton, J., Bosma, G., and Lieber, M.R. (1992). Analysis of the defect in DNA end joining in the murine *scid* mutation. Mol. Cell. Biol. *12*, 4758–4768.

Hendrickson, E.A., Qin, X.-Q., Bump, E.A., Schatz, D.G., Oettinger, M., and Weaver, D.T. (1991). A link between double-strand break-related repair and V(D)J recombination: the *scid* mutation. Proc. Natl. Acad. Sci. USA *88*, 4061–4065.

Henriques, J.A., and Moustacchi, E. (1980). Isolation and characterization of pso mutants sensitive to photo-addition of psoralen derivatives in *Saccharomyces cerevisiae*. Genetics *95*, 273–288.

Hiom, K., and Gellert, M. (1997). A stable RAG1–RAG2-DNA complex that is active in V(D)J cleavage. Cell *88*, 65–72.

Howard, F.B., Chen, C.Q, Ross, P.D., and Miles, H.T. (1991). Hairpin formation in the self-complementary dodecamer d-GGTACGCG TACC and derivatives containing GA and IA mispairs. Biochemistry *30*, 779–782.

Kowalczykowski, S.C., and Eggleston, A.K. (1994). Homologous pairing and DNA strand-exchange proteins. Annu. Rev. Biochem. *63*, 991–1043.

Leuther, K.K., Hammarsten, O., Kornberg, R.D., and Chu, G. (1999). Structure of DNA-dependent protein kinase: implications for its regulation by DNA. EMBO J. *18*, 1114–1123.

Lewis, S.M. (1994). The mechanism of V(D)J joining: lessons from molecular, immunological and comparative analyses. Adv. Immunol. *56*, 27–150.

Lieber, M.R. (1991). Site-specific recombination in the immune system. FASEB J. *5*, 2934–2944.

Lieber, M.R. (1997). The FEN-1 family of structure-specific nucleases in eukaryotic DNA replication, recombination, and repair. Bioessays *19*, 233–240.

Lieber, M.R. (1998). Pathological and physiological double-strand breaks: roles in cancer, aging, and the immune system. Am. J. Pathol. *153*, 1323–1332.

Lieber, M.R. (1999). The biochemistry and biological significance of nonhomologous DNA end joining: an essential repair process in multicellular eukaryotes. Genes Cells *4*, 77–85.

Lieber, M.R., Hesse, J.E., Lewis, S., Bosma, G.C., Rosenberg, N., Mizuuchi, K., Bosma, M.J., and Gellert, M. (1988). The defect in murine severe combined immune deficiency: joining of signal sequences but not coding segments in V(D)J recombination. Cell *55*, 7–16.

Lobachev, K.S., Gordenin, D.A., and Resnick, M.A. (2002). The mre11 complex is required for repair of hairpin-capped double-strand breaks and prevention of chromosome rearrangements. Cell *108*, 183–193.

Ma, Y., and Lieber, M.R. (2001). DNA length-dependent cooperative interaction in the binding of Ku to DNA. Biochemistry *40*, 9638–9646.

Ma, Y., and Lieber, M.R. (2002). Binding of inositol hexakisphosphate (IP6) to Ku but not to DNA-PK$_{cs}$. J. Biol. Chem. *277*, in press.

McCormack, W.T., Tjoelker, L.W., Carlson, L.M., Petryniak, B., Barth, C.F., Humphries, E.H., and Thompson, C.B. (1989). Chicken IgL gene rearrangement involves deletion of a circular episome and addition of single nonrandom nucleotides to both coding segments. Cell *56*, 785–791.

Modesti, M., Hesse, J.E., and Gellert, M. (1999). DNA binding of Xrcc4 protein is associated with V(D)J recombination but not with stimulation of DNA ligase IV activity. EMBO J. *18*, 2008–2018.

Moshous, D., Li, L., de Chasseval, R., Philippe, N., Jabado, N., Cowan, M.J., Fischer, A., and de Villartay, J.-P. (2000). A new gene involved in DNA double-strand break repair and V(D)J recombination is located on human chromosome 10p. Hum. Mol. Genet. *9*, 583–588.

Moshous, D., Callebaut, I., de Chasseval, R., Corneo, B., Cavazzana-Calvo, M., Le Diest, F., Tezcan, I., Sanal, O., Bertrand, Y., Philippe, N., et al. (2001). Artemis, a novel DNA double-strand break repair/V(D)J recombination protein, is mutated in human severe combined immune deficiency. Cell *105*, 177–186.

Nicolas, N., Moshous, D., Cavazzana-Calvo, M., Papadoupoulo, D., de Chasseval, R., Le Deist, F., Fischer, A., and de Villartay, J.-P. (1998). A human severe combined immunodeficiency (SCID) condition with increased sensitivity to ionizing radiations and impaired V(D)J rearrangements defines a new DNA recombination/repair deficiency. J. Exp. Med. *188*, 627–634.

Paul, W. (1999). Fundamental Immunology, 4th Edition (New York: Raven Press).

Paull, T.T., and Gellert, M. (1998). The 3′ to 5′ exonuclease activity of Mre11 facilitates repair of DNA double-strand breaks. Mol. Cell *1*, 969–979.

Paull, T.T., and Gellert, M. (1999). Nbs1 potentiates ATP-driven DNA unwinding and endonuclease cleavage by the Mre11/Rad50 complex. Genes Dev. *13*, 1276–1288.

Raghunathan, G., Jernigan, R.L., Miles, H.T., and Sasisekharan, V. (1991). Conformational feasibility of a hairpin with two purines in the loop. 5′-d-GGTAC*IA*GTACC-3′. Biochemistry *30*, 782–788.

Roth, D.B., Menetski, J.P., Nakajima, P., Bosma, M.J., and Gellert, M. (1992). V(D)J recombination: broken DNA molecules with covalently sealed (hairpin) coding ends in scid mouse thymocytes. Cell *70*, 983–991.

Schar, P., Herrmann, G., Daly, G., and Lindahl, T. (1997). A newly identified DNA ligase of *Sacchromyces cerevisiae* involved in RAD52-independent repair of DNA double-strand breaks. Genes Dev. *11*, 1912–1924.

Schlissel, M.S. (1998). Structure of nonhairpin coding-end DNA breaks in cells undergoing V(D)J recombination. Mol. Cell. Biol. *18*, 2029–2037.

Schuler, W., Weiler, I.J., Schuler, A., Phillips, R.A., Rosenberg, N., Mak, T.W., Kearney, J.F., Perry, R.P., and Bosma, M.J. (1986). Rearrangement of antigen receptor genes is defective in mice with severe combined immune deficiency. Cell *46*, 963–972.

Schwarz, K., Hansen-Hagge, T.E., Knobloch, C., Friedrich, W., Kleihauer, E., and Bartram, C.R. (1991). Severe combined immunodeficiency (SCID) in man: B cell-negative (B-) SCID patients exhibit an irregular recombination pattern at the J$_H$ locus. J. Exp. Med. *174*, 1039–1048.

Schwarz, K., Gauss, G.H., Ludwig, L., Pannicke, U., Li, Z., Lindner, D., Friedrich, W., Seger, R.A., Hansen-Hagge, T.E., Desiderio, S., et al. (1996). RAG mutations in human B cell-negative SCID. Science *274*, 97–99.

Shen, B., Nolan, J.P., Sklar, L.A., and Park, M.S. (1996). Essential amino acids for substrate binding and catalysis of human flap endonuclease 1. J. Biol. Chem. *271*, 9173–9176.

Teo, S.H., and Jackson, S.P. (1997). Identification of *Saccharomyces cerevisiae* DNA ligase IV: involvement in DNA double-strand break repair. EMBO J. *16*, 4788–4795.

Vanasse, G.J., Concannon, P., and Willerford, D.M. (1999). Regulated genomic instability and neoplasia in the lymphoid lineage. Blood *94*, 3997–4010.

van Gent, D.C., Mizuuchi, K., and Gellert, M. (1996). Similarities between initiation of V(D)J recombination and retroviral integration. Science *271*, 1592–1594.

van Gent, D.C., Hoeijmakers, J.H.J., and Kanaar, R. (2001). Chromosomal stability and the DNA double-stranded break connection. Nat. Rev. Genet. *2*, 196–206.

Villa, A., Sobacchi, C., Notarangelo, L.D., Bozzi, F., Abinun, M., Abrahamsen, T.G., Arkwright, P.D., Baniyash, M., Brooks, E.G., Conley, M.E., et al. (2001). V(D)J recombination defects in lymphocytes due to RAG mutations: severe immunodeficiency with a spectrum of clinical presentations. Blood *97*, 81–88.

Walker, J.R., Corpina, R.A., and Goldberg, J. (2001). Structure of the Ku heterodimer bound to DNA and its implications for double-strand break repair. Nature *412*, 607–614.

West, R.B., Yaneva, M., and Lieber, M.R. (1998). Productive and nonproductive complexes of Ku and DNA-dependent protein kinase at DNA termini. Mol. Cell. Biol. *18*, 5908–5920.

West, C.E., Waterworth, W.M., Jiang, Q., and Bray, C.M. (2000). *Arabidopsis* DNA ligase IV is induced by gamma-irradiation and interacts with an *Arabidopsis* homologue of the double-strand break repair protein XRCC4. Plant J. *24*, 67–78.

Wilson, T.E., and Lieber, M.R. (1999). Efficient processing of DNA ends during yeast nonhomologous end joining. Evidence for a DNA polymerase beta (Pol4)-dependent pathway. J. Biol. Chem. *274*, 23599–23609.

Wilson, T.E., Grawunder, U., and Lieber, M.R. (1997). Yeast DNA ligase IV mediates non-homologous DNA end joining. Nature *388*, 495–498.

Wood, R.D., Mitchell, M., Sgouros, J., and Lindahl, T. (2001). Human DNA repair genes. Science *291*, 1284–1289.

Wu, X., Wilson, T.E., and Lieber, M.R. (1999). A role for FEN-1 in

nonhomologous DNA end joining: the order of strand annealing and nucleolytic processing events. Proc. Natl. Acad. Sci. USA *96*, 1303–1308.

Xie, Y., Liu, Y., Argueso, J.L., Henricksen, L.A., Kao, H.I., Bambara, R.A., and Alani, E. (2001). Identification of rad27 mutations that confer differential defects in mutation avoidance, repeat tract instability, and flap cleavage. Mol. Cell. Biol. *21*, 4889–4899.

Yaneva, M., Kowalewski, T., and Lieber, M.R. (1997). Interaction of DNA-dependent protein kinase with DNA and with Ku: biochemical and atomic-force microscopy studies. EMBO J. *16*, 5098–5112.

Yeo, T.C., Xia, D., Hassouneh, S., Yang, X.O., Sabath, D.E., Sperling, K., Gatti, R.A., Concannon, P., and Willerford, D.M. (2000). V(D)J rearrangement in Nijmegen breakage syndrome. Mol. Immunol. *37*, 1131–1139.

Zhu, C., Bogue, M.A., Lim, D.-S., Hasty, P., and Roth, D.B. (1996). Ku86-deficient mice exhibit severe combined immunodeficiency and defective processing of V(D)J recombination intermediates. Cell *86*, 379–389.